REPORT DOCUMENTATION PAGE

Form Approved OMB No. 0704-0188

1. REPORT DATE *(DD-MM-YYYY)*	2. REPORT TYPE	3. DATES COVERED *(From – To)*
27-02-2003	Final Report	21 September 2001 - 21-Mar-02

4. TITLE AND SUBTITLE

Aging Properties of An HTPB Propellant

5a. CONTRACT NUMBER
F61775-01-WE072

5b. GRANT NUMBER

5c. PROGRAM ELEMENT NUMBER

6. AUTHOR(S)

Dr. Robert Neviere

5d. PROJECT NUMBER

5d. TASK NUMBER

5e. WORK UNIT NUMBER

7. PERFORMING ORGANIZATION NAME(S) AND ADDRESS(ES)
SNPE
2 rue Lavoisier
Vert-le-Petit BP2 91710
France

8. PERFORMING ORGANIZATION REPORT NUMBER

N/A

9. SPONSORING/MONITORING AGENCY NAME(S) AND ADDRESS(ES)

EOARD
PSC 802 BOX 14
FPO 09499-0014

10. SPONSOR/MONITOR'S ACRONYM(S)

11. SPONSOR/MONITOR'S REPORT NUMBER(S)
SPC 01-4072

12. DISTRIBUTION/AVAILABILITY STATEMENT

Approved for public release; distribution is unlimited.

13. SUPPLEMENTARY NOTES

14. ABSTRACT

The mechanical properties of an HTPB propellant are observed during the ageing process of this material including diiferent conditions of temperature and humidity. The report concerns the results of initial time and after an ageing duration of 6 months under conditions of +50°C and +20°C for relative humidity of Hr76%, Hr33% and in dry air. The mechanical properties observed are more precisely the crack propagation capabilty of the material but for modelisation and numerical calculation purposes, the material is also tested in uniaxial tension at different strain rates, in simple shear for one strain rate and in the volumetric characterisation test (uniaxial tension in the Farris gaz dilatometer) for different strain rates. To allow a complete viscoelastic description, the material is also tested in the uniaxial tension relaxation test for different imposed elongations. The program scope is to perform a crack propagation numerical simulation in the Air Force Research Laboratory using the high performance numerical tools available there for an SNPE formulated material.

15. SUBJECT TERMS
EOARD, Solid Fuels, Propellants, aging propellants

16. SECURITY CLASSIFICATION OF:			17. LIMITATION OF ABSTRACT	18, NUMBER OF PAGES	19a. NAME OF RESPONSIBLE PERSON
a. REPORT	b. ABSTRACT	c. THIS PAGE			INGRID J. WYSONG
UNCLAS	UNCLAS	UNCLAS	UL	23	19b. TELEPHONE NUMBER *(Include area code)* +44 (0)20 7514 4285

SNPE Propulsion
GROUPE SNPE
Centre de recherche du BOUCHET
Laboratoire de mécanique expérimentale TCFM

Ageing properties of an PBHT propellant

PV n° 21/CRB-DFP-TCFM/2002

du 20-04-2002

Monique LUCAS
Robert NEVIERE

Rédacteur	Vérificateur
R.Nevière M.Lucas	Robert Nevière

Acknowledgment and support: This material is based upon work supported by the European Office of Aerospace Research and Development, Air Force Office of Scientific Research, Air Force Laboratory, under contract F61775-01-WE072.

Any opinions, findings and conclusions or recommendations expressed in this material are those of the authors and do not necessarily reflect the views of the European Office

of Aerospace Research and Development, Air Force Office of Scientific Research, Air Force Laboratory.

SME hereby declares that, to the best of its knowledge and belief, the technical data delivered herewith under Contract No. F61775-01-WE072 is complete, accurate, and complies with all requirements of the contract."

I certify that there were no subject inventions to declare as defined in FAR 52.227-13, during the performance of this contract."

DATE: 28 Octobre 2003
Name and Title of Authorized Official: Robert NEVIERE

Destinataires : CRB : TCFM
AFRL : Jimmy LIU

1. Introduction

The mechanical properties of an HTPB propellant is observed during the ageing process of this material including diiferent conditions of temperature and humidity. The report concerns the results of initial time and after an ageing duration of 6 months under conditions of +50°C and +20°C for relative humidity of Hr76%, Hr33% and in dry air. The mechanical properties observed are more precisely the crack propagation capabilty of the material but for modelisation and numerical calculation purposes, the material is also tested in uniaxial tension at different strain rates, in simple shear for one strain rate and in the volumetric characterisation test (uniaxial tension in the Farris gaz dilatometer) for different strain rates. To allow a complete viscoelastic description, the material is also tested in the uniaxial tension relaxation test for different imposed elongations. The program scope is to perform a crack propagation numerical simulation in the Air Force Research Laboratory using the high performance numerical tools available there for an SNPE formulated material.

2. Material ageing conditions

The material a typical HTPB propellant is aged in sealed cases containing different salted solutions from which a determined relative humidy control is expected. The sealed cases are placed in air temperature controled chambers during the ageing duration. The different ageing conditions are recalled in table 1.

atmosphere	temperature	relative humidity	ageing duration	ageing duration
air	+20°C	dry		6 months
air	+20°C	33%		6 months
air	+20°C	76%		6 months
air	+50°C	dry	to	6 months
air	+50°C	33%		6 months
air	+50°C	76%		6 months

Table 1 : Ageing conditions and durations

All tests are conducted rapidly without a dessication procedure, the material is thus assuled to be in equilibrium with the humidity of the sealed case.

3. Material testing at initial time

3.1 Dynamic Mechanical Analysis

The first characterisation of viscoelastic materials consist in the convenient experiment of Dynamic Mechanical Analysis (DMA) from which the shifting factors of the time-temperature superposition principle may be extracted. The HTPB material involved in this study was thus tested using this technique for 3 frequencies and a temperature range of +60°C to -80°C. The samples are small rectangular bars of 10x5x25mm to which is applied a continue cooling at the rate of -2°C/min to insure a permanent temperature equilibrium. The excitation signal of a constant frequence (7.8-32.5 and 125Hz) is displacement controlled with an amplitude of 10µm (0.04% strain). The figure 1 shows the the real modulus for the 3 frequencies on the entire temperature domain while the figure 2 shows the same results in terms of loss tangent.

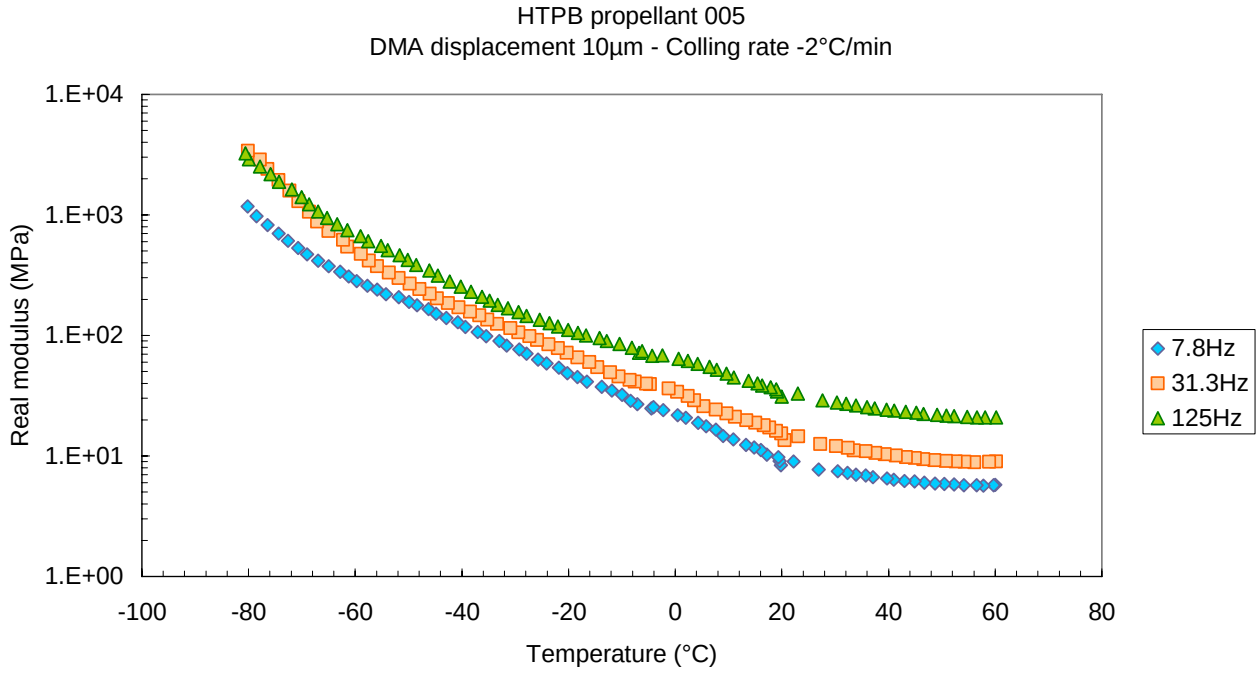

Figure 1 : Real modulus for 3 frequencies

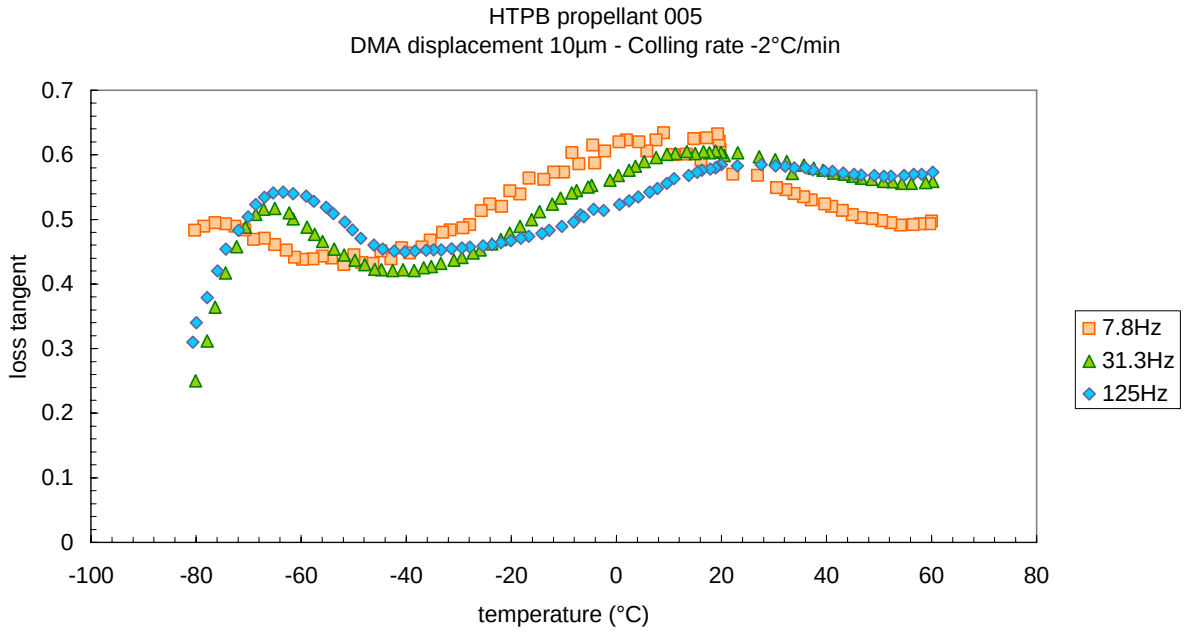

Figure 2 : dissipation spectrum for 3 frequencies

The results are typical of an HTPB proppelant with two specific dissipation peaks recorded on the loss tangent. The first of them located between -60°C and -80°C depending on the frequence is attributed to the glass transition while the second one, at a much higher temperature, which also frequency dependant, is knowned to be characteristic of the free macromolecules movments in the elastomeric network.

From these isochrones results one may easely select isotherms from which it is then possible to derive the shift factors of the time-temperature equivalency. This was done on these specific results with unexpected difficulty to give the factors of figure 3 which are then fitted with the WLF relationship allowing the ulterior use in the master curves constructions for others mechanical properties.

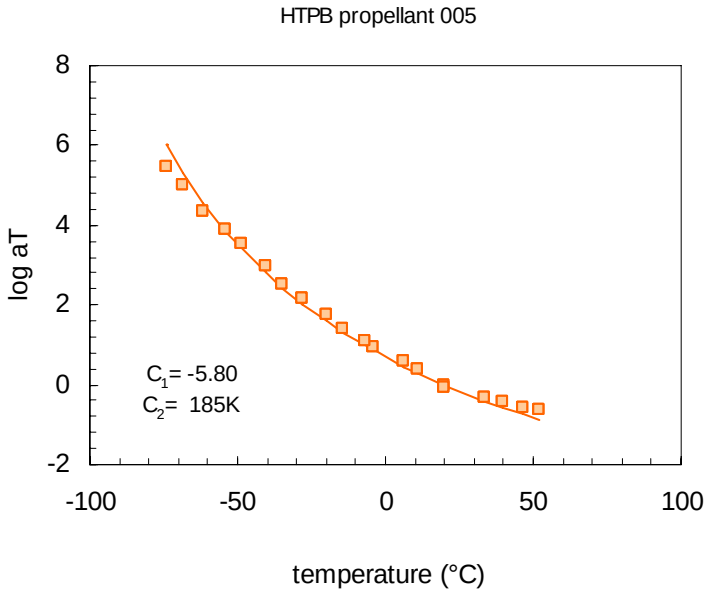

Figure 3 : time-temperature equivalency shift factors.

3.2 Uniaxial tension at constant strain rate

Since the program concerns a viscoelastic description of the behaviour, the material was tested for different strain rates and temperatures. For the initial time the results have been extended to these different conditions but due to the poor quantity of material available for this program, the complete characterisation could not be extended so much at every observed ageing duration.

The properties are first measured in a conventional uniaxial tension test at constant strain rate. The sample geometry is a modified Jannaf sample depicted on figure 4 for which the equivalent length is 115mm. The main modification concerns the application of the displacement as boundaries conditions to the sample. This modification consist in changing from a slippery system to a bonded system.

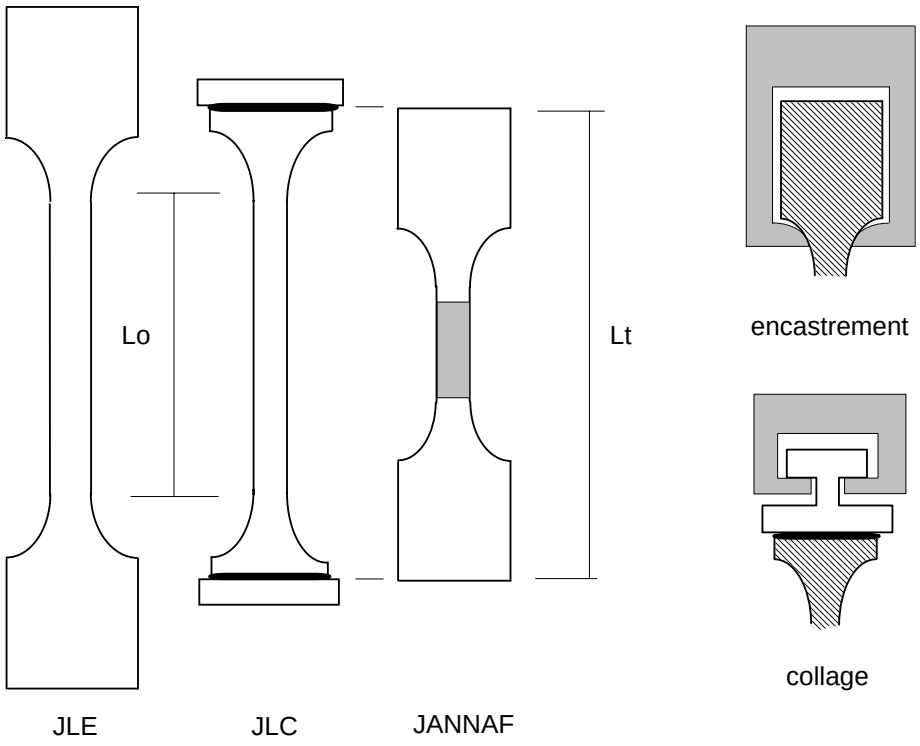

Figure 4 : Modified Jannaf sample

With this sample geometry, the crosshead speed is chosen to give decimal values of the strain rate of 0.1-10 and 4.5 min^{-1} (11.5-115 and 500mm/min this latter being the upper range of the dynamometer capability). For the initial time, the tests are extended to a temperature range lying between -20°C and +60°C for the single crosshead speed of 115mm/min. Since the time-temperature shift factors are known from the DMA experiments, the results may be presented as a master curve portion. The results in terms of stress-strain relationships for the different tested temperatures are shown on figure 5 for the initial time and on figure 6 for the different strain rates at the temperature of +20°C. The accidental response at -20°C is due to the presence of some ice around the shaft of the machine which was not detected during the test and pertubated the crosshead displacement.

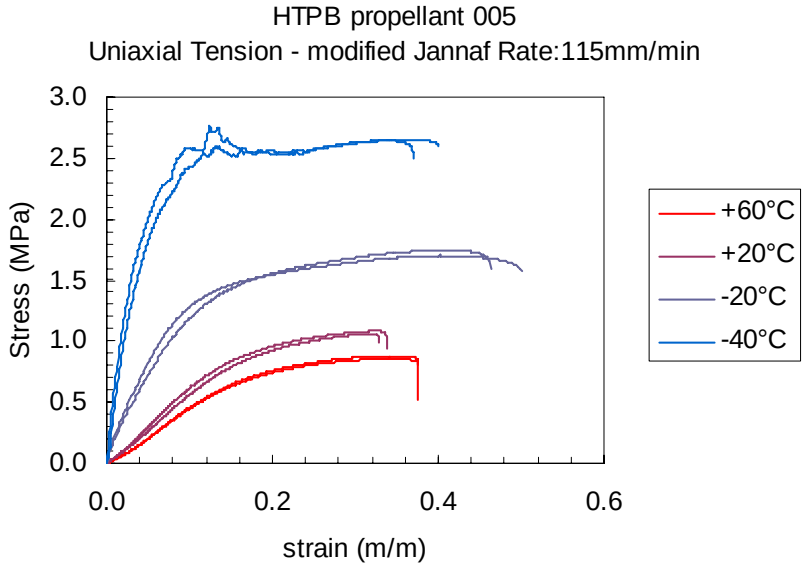

Figure 5 : uniaxial tensile tests at different temperatures

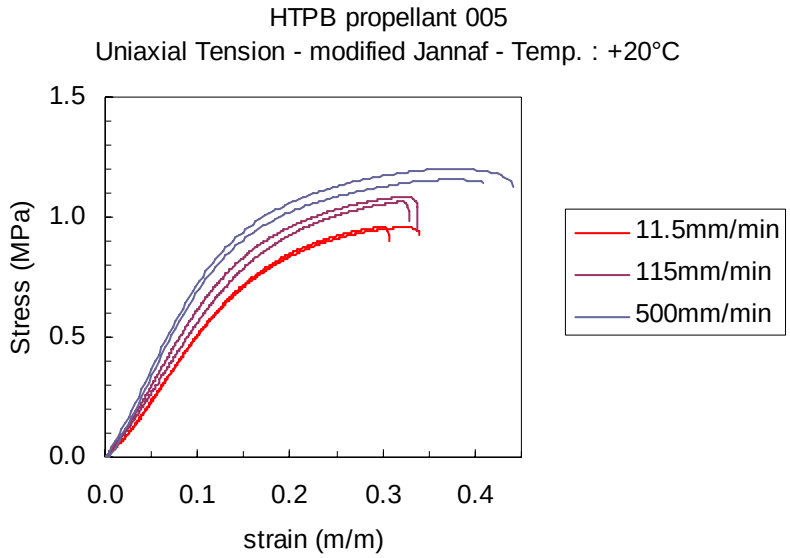

Figure 6 : uniaxial tensile tests at different rates

From this set of results one may extract the following standard properties which are defined as the maximum rigidity modulus (in the pseudo linear region), the maximum stress S_m , the associated strain e_m at that stress and finaly the ultimate strain at fracture ε_r. These values are reminded in table 2 and are the input to the construction of the master curves portions shown on figure 7.

ageing duration	ageing temp.	relative humidity	test temp.	strain rate	E_{tg}	S_m	e_m	e_r
months	°C	%	°C	min^{-1}	MPa	MPa	%	%
initial	-	-	60	1	5.1	0.88	33.3	37.4
			60	1	5.0	0.85	32.7	37.5
initial	-	-	20	0.1	5.7	0.95	28.4	30.7
			20	0.1	5.6	0.95	31.2	33.8
initial	-	-	20	1	6.7	1.08	31.2	33.7
			20	1	6.1	1.06	31.0	32.8
initial	-	-	20	4.35	7.9	1.2	36.5	43.8
			20	4.35	7.9	1.15	35.5	40.9
initial	-	-	-20	1	23.0	1.71	40.3	49.8
			-20	1	21.0	1.75	39.8	45.8
initial	-	-	-40	1	48.4	2.66	33.3	37.0
			-40	1	68.4	2.65	35.6	40.0

Table 2 : Uniaxial tensile properties

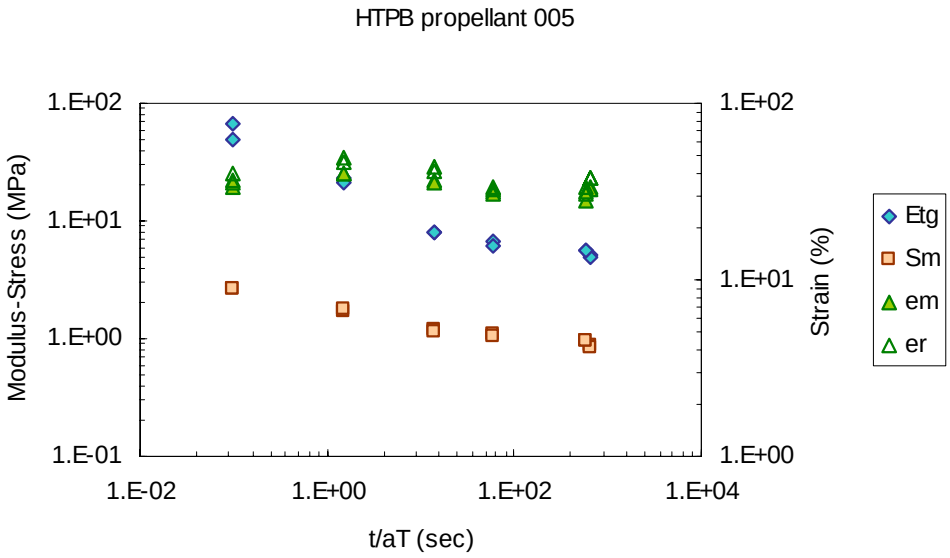

Figure 7 : Master curves of the tensile properties

3.3 Uniaxial tension relaxation tests

In addition to these tests, the material behaviour is also observed in uniaxial relaxation experiments. Three strain level are achieved, namely 5%, 10% and 15%. The stress relaxation is recorded during 6000 seconds (100min). The recorded stress versus time is shown on figure 8.

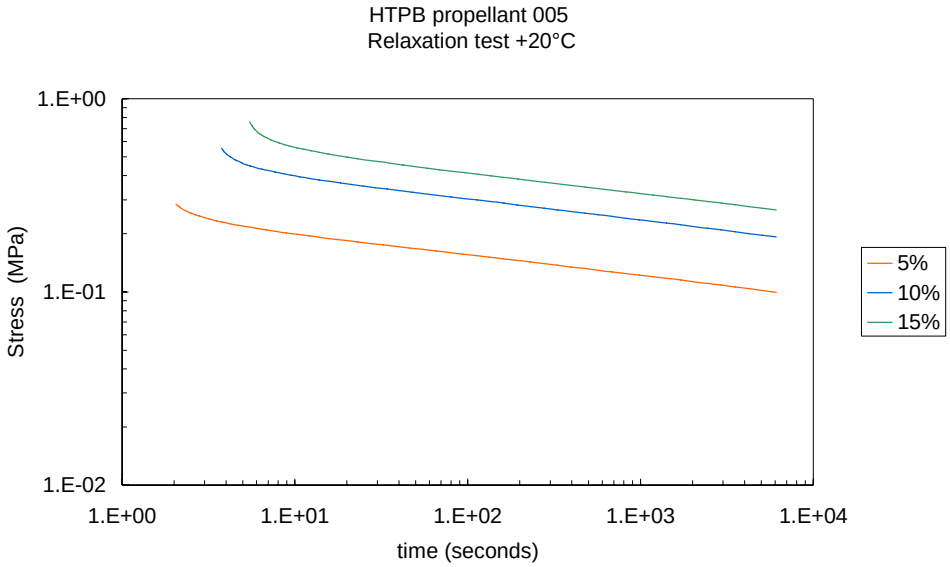

Figure 8 : Stress relaxation for 3 strains

It is of concern to point out the large difference commonly observed between the uniaxial tensile test modulus and the relaxation modulus. This difference is due to the strong non linear viscoelastic effects which are revealed by the fact that the relaxation modulus falls very rapidly as soon as the deformation applied to the sample no longer increases. Then, if one plots on the same graph, as on figure 9, the relaxation and tensile modulus the difference is obvious even if the definition of time is not common in these experiments.

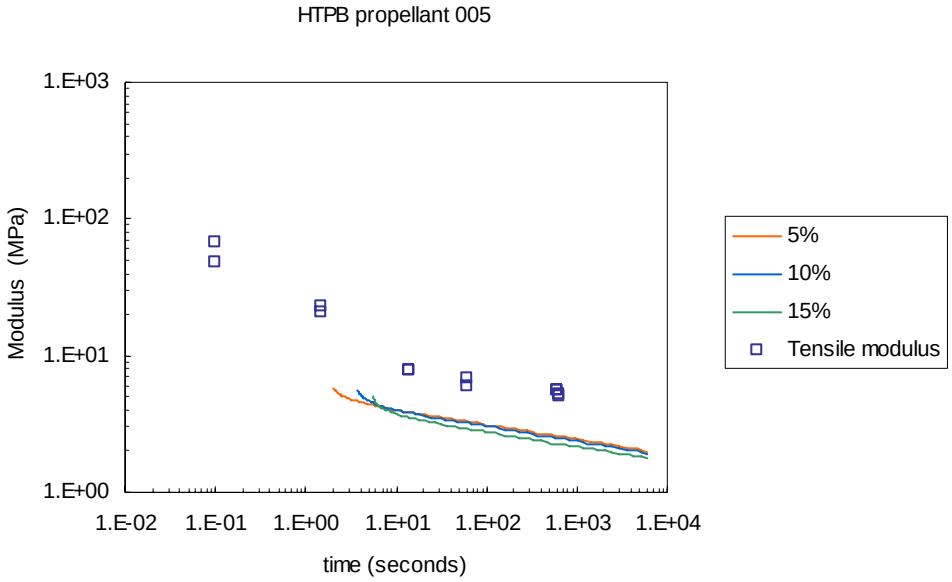

Figure 9 : Relaxation and tensile modulus

3.4 Volume dilatation test

The volume dilatation is of course of main importance despite the fact that numerical simulations are generally incompressible. This material property may be measured in the Farris gaz dilatometer during a tensile test. To remind the principle of the Farris gaz dilatometer, the figure 10 shows a functioning scheme

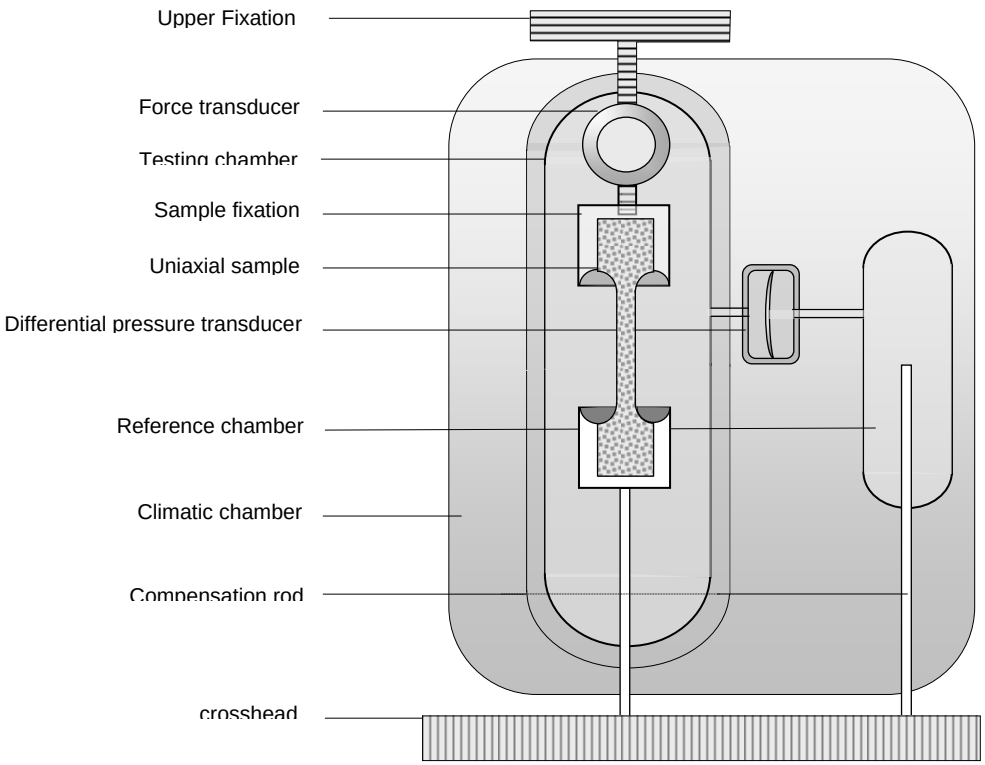

Figure 10 : Farris gaz dilatometer

The material has been tested in the dilatometer at the ambiant temperature and 3 crosshead speed (5- 50 - 500mm/min) . The samples are conventionnal Jannaf geometry but the dogbone heads are cut off to reduce the fixation apparatus overall dimensions. The results in terms of tensile properties are coherent with the previous experiments as shown on the master curves of figure 11.

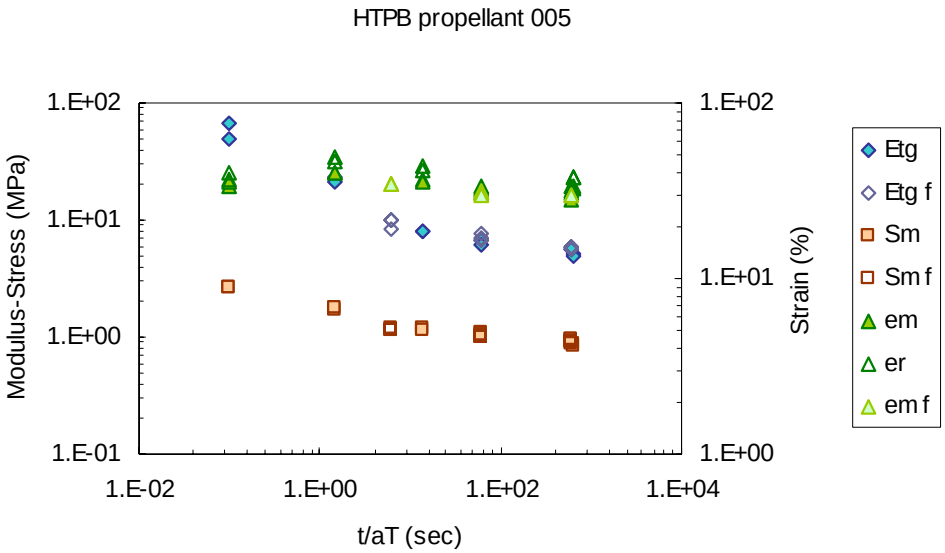

Figure 11 : tensile properties from Farris gaz dilatometer (*noted f*)

The material response in terms of volume dilatation is shown on figure 12.

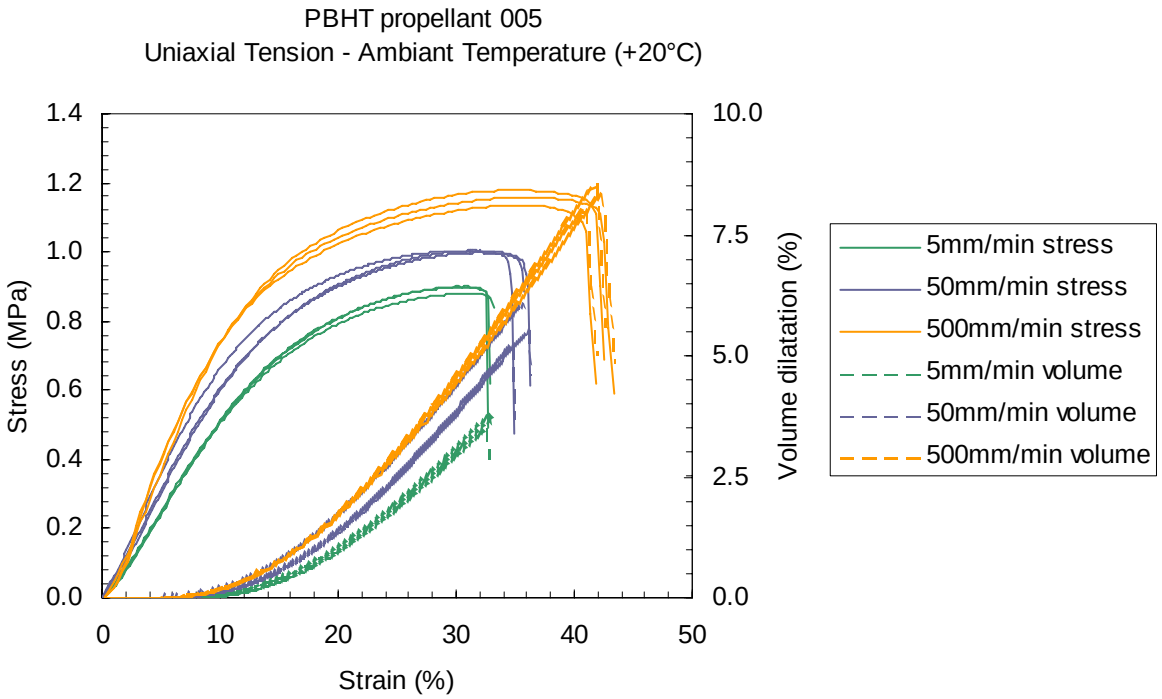

Figure 12 : Farris gaz dilatometer characterization

The results are typical of an HTPB propellant with an incompressible domain up to 10% at least varying slightly with the strain rate. Overpassing this domain, the volume increases rapidly before reaching a zero creation rate of voids (a linear domain of variation of the global volume). The slope which is characteristic of this domain is also slightly rate dependant.

3.5 Simple shear tensile tests

An hyperelastic ajustment on the results in the initial condition was performed with the intention to help as a guide for the construction of more realistic constitutive material laws (viscoelastic). To obtain a confident fitting process a simple shear experiment is added to the material data at the unique strain rate of $1min^{-1}$ but for different temperatures. The sample are composed of 2 rectangular plates of 5mm thickness and 50x50mm² section bonded to strong metallic supports in order to respect the boundaries conditions of fixed dispacement on the surfaces. The results to such experiments is presented on the figure 13.

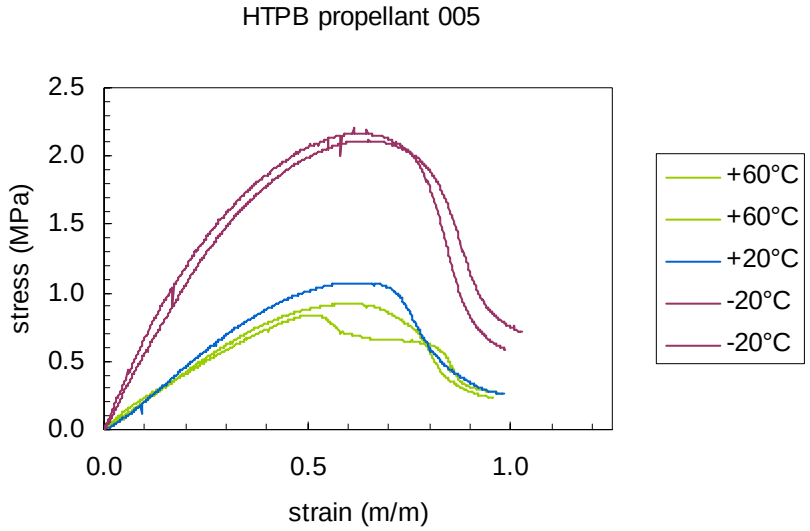

Figure 13 : Simple shear experiments

Once this results are available the fitting process to obtain hyperelastic models is easely performed using a very conventionnal least square technique. The hyperelastic strain energy potential is developped up to order 2 but only four terms were retained :

$$W_{el} = \sum_{i+j=1}^{2} C_{ij} \cdot (I_1 - 3)^i (I_2 - 3)^j \qquad \text{with} \quad C_{11} = 0$$

The fittings of this model to experimental uniaxial and shear results are presented on figure 14.

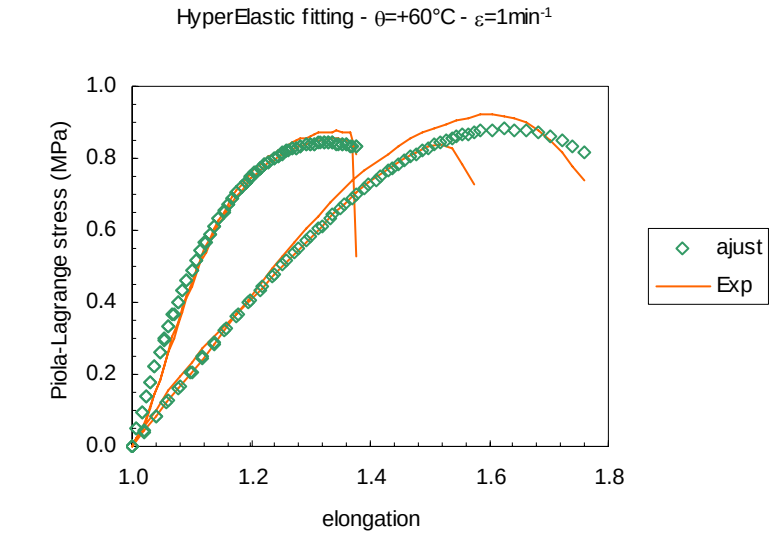

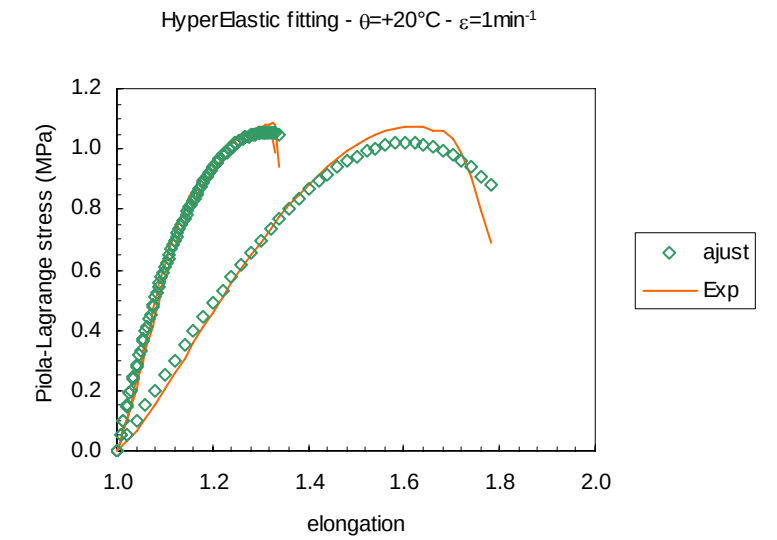

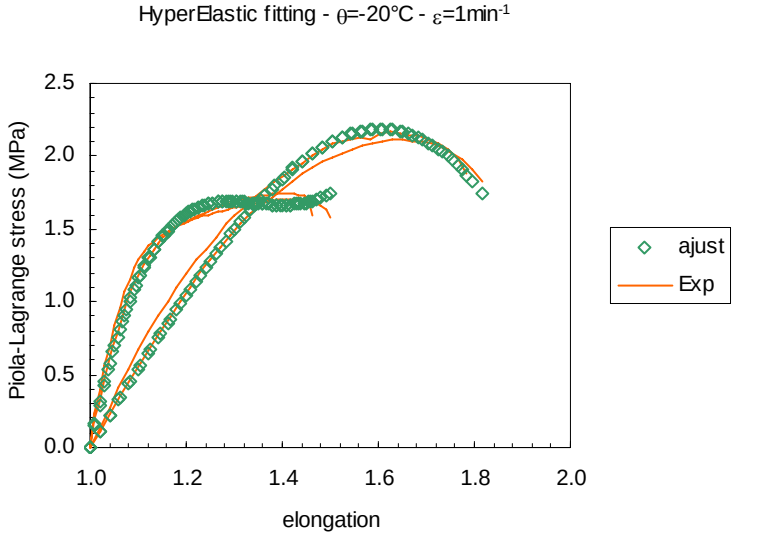

Figure 14 : Hyperelastic fittings

It is worthnotting that coefficients of the hyperelastic laws seems to vary with a coherent sense with the reduced temperature as shown on figure 15.

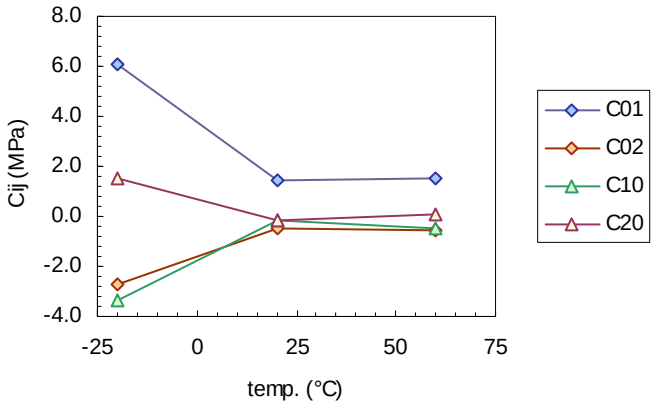

Figure 15 : temperature dependance of the Hyperelastic fitting coefficients

θ=	60	20	-20
C_{01}=	1.50	1.43	6.06
C_{02}=	-0.54	-0.44	-2.74
C_{10}=	-0.44	-0.17	-3.35
C_{20}=	0.09	-0.13	1.51

Table3 : Hyperelastic coefficients values

3.6 Crack propagation tests

All these cumulated experimental results gives a clear picture of the material behaviour, it is now time to turn to the observation of the true target of this work : the crack propagation tests. Two geometries were tested in a single sample geometry of 5x110x20mm namely the SENT and the pure shear (PS). The figure 16 shows schematically the samples geometry and boudaries conditions.

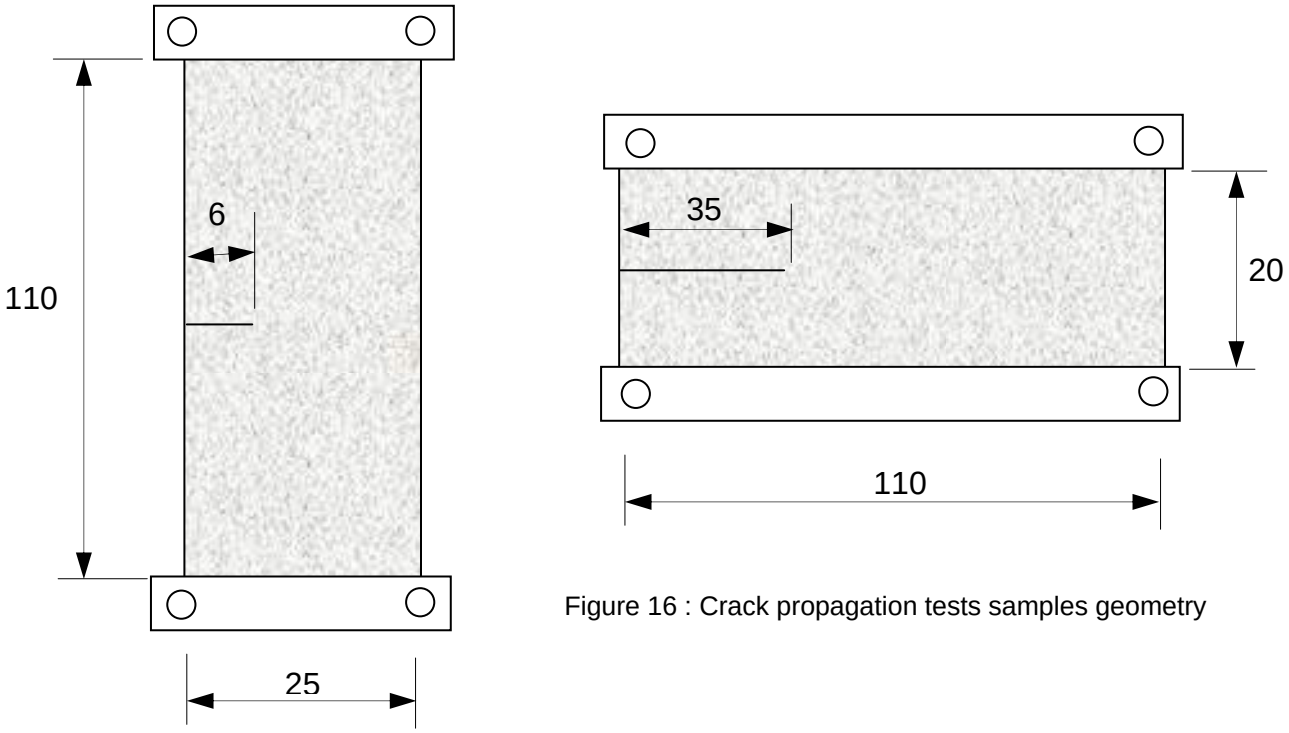

Figure 16 : Crack propagation tests samples geometry

The experiments are all conducted at room temperature and to a rate in proportion with the sample height which leads to respectively to 25mm/min for the SENT samples and 5mm/min for the PS samples. The propagation of the crack is recorded using a synchroneous video set up with an integrated clock as shown on figure 17.

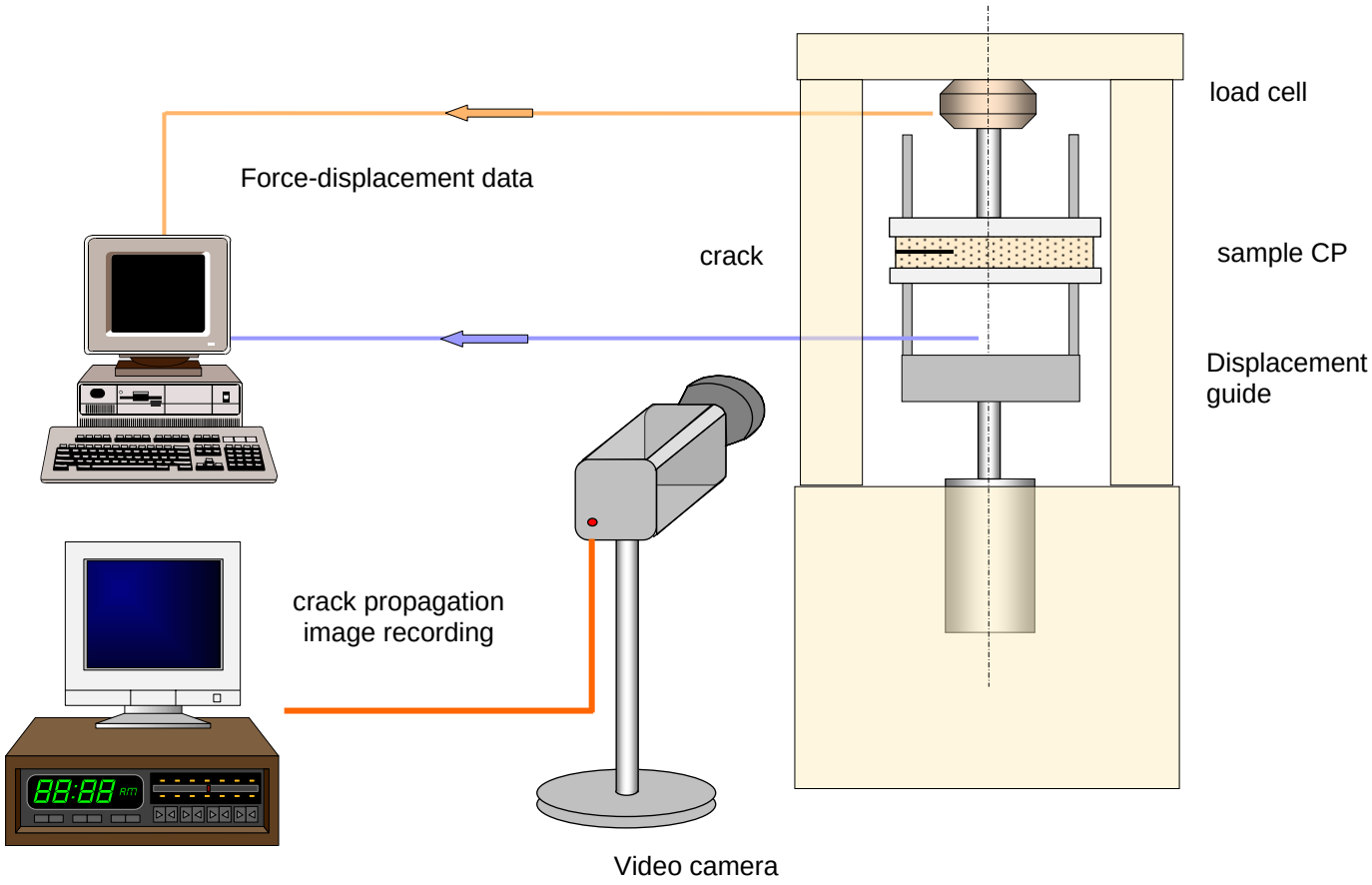

Figure 17 : Synchroneous video crack propagation recordings

From this recordings and with the simultaneaous load-displacement trace, one is able to evaluate the critical stress-intensity factor and the crack propagation speed.

These measures leads to the graphs displacement-load-crack length shown on figure 18 and 19 respectively for the SENT and the PS specimens.

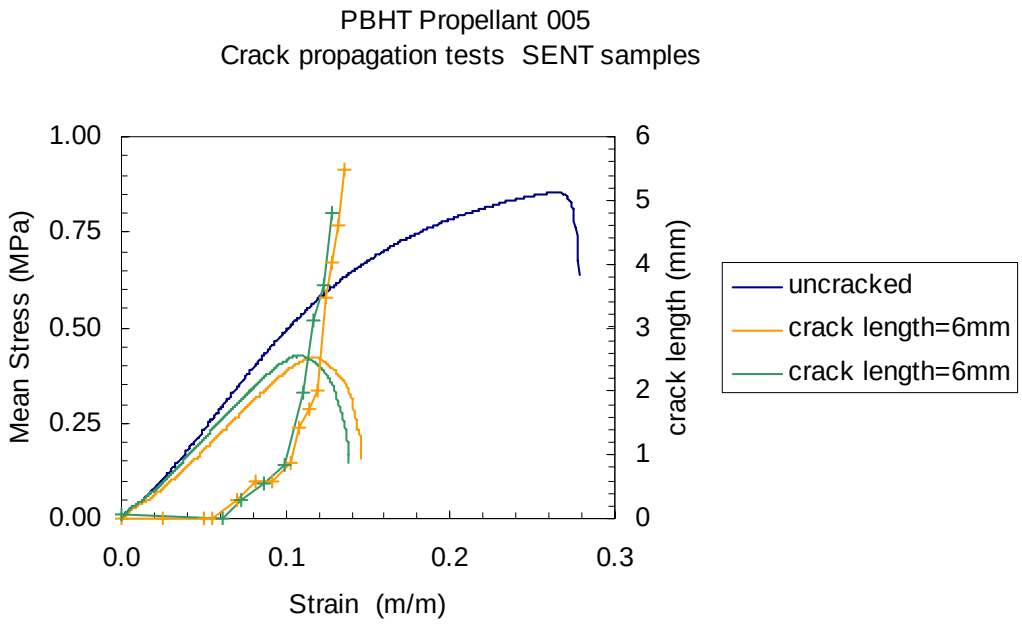

Figure 18 : crack propagation recordings for SENT specimens (θ=+20°C R=25mm/min)

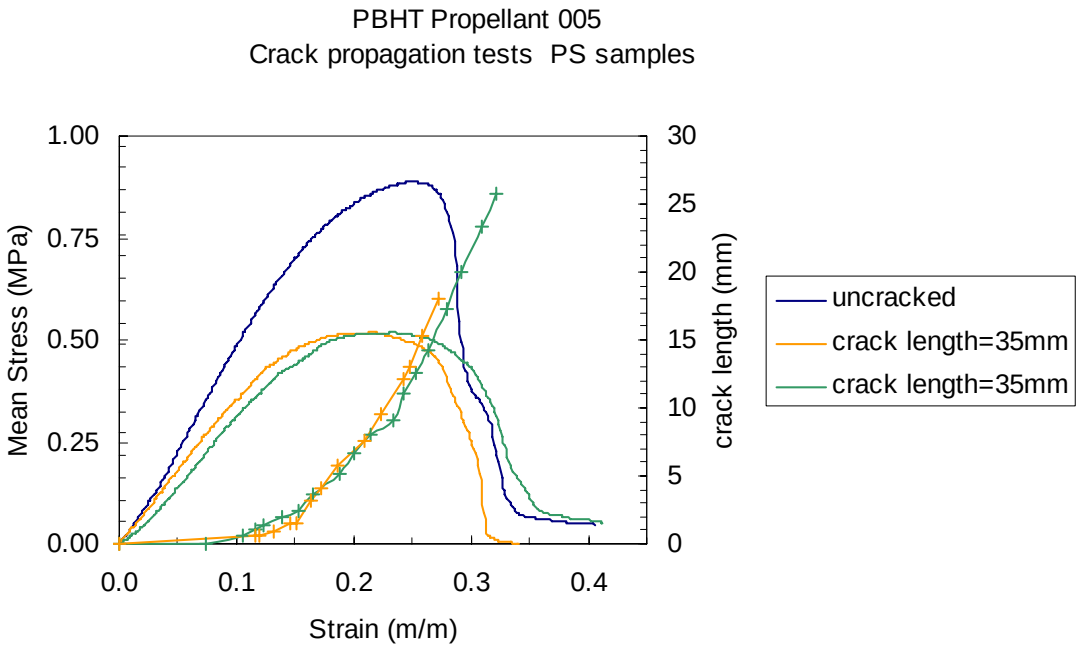

Figure 19 : crack propagation recordings for PS specimens (θ=+20°C R=5mm/min)

From the recording of the fracture load at the instant of propagation onset, it is possible to evaluate both a critical stress intensity factor, K_{1c}, and a fracture energy, G_c. The conventionnal fracture mechanics relations used to derive these values are for the critical stress intensity factor in the PS samples :

$$K_{1c} = \sigma_c . \sqrt{\frac{3}{8} h}$$

where σ_c is the critical ligament stress and h the undeformed height of the sample. For the facture energy the relation is simply :

$$G_c = \frac{K_{1c}^2}{E}$$

For the SENT samples the linear elastic analysis provides :

$$K_{1c} = \sigma_0 . \sqrt{\pi a} . Y(a, h, B)$$

where σ_0 is the stress in the region far from the crack tip where it is uniform, a the crack length and Y a correcting function to take into account for the boundaries conditions which value for short cracks may be taken as 1,12. In terms of fracture energy, the analysis due to GreenSmith and Thomas leads to :

$$G_c = k(\lambda) . W_O . a$$

A correction factor may be added to the expression in the form of Y^2. We have prefered to use once again the linear fracture mechanics relation for reasons of simplicity :

$$G_c = \frac{K_{1c}^2}{E}$$

Table 4 gives the values extracted from the experiments (modulus is considered as 5.4MPa)

sample	a_0	h_0	σ_c	K_{1c}	G_c
	mm	mm	MPa	MPa$\sqrt{m}$	mJ/mm²
SENT	6	110	0.313	0.048	0.430
SENT	6	110	0.273	0.042	0.326
PS	35	21	0.612	0.054	0.547
PS	35	21	0.526	0.047	0.403

Table 4 : Crack propagation initiation properties

Both geometries gives comparble values but the better result is obtained with the fracture energy measurements, G_c, as could be expected from its non linear nature.

4. Properties of aged propellant

4.1 Mechanical spectroscopy

A low cost method to observe the ageing process of propellant and generally of polymers, is obviously the DMA technique and more precisely the observation of the dissipation properties (loss tangent). The aged HTPB material was tested using this technique as in §3.1 but for the unique frequency of 7.8Hz. The results are presented in termes of real modulus and loss tangent on figures 20 and 21.

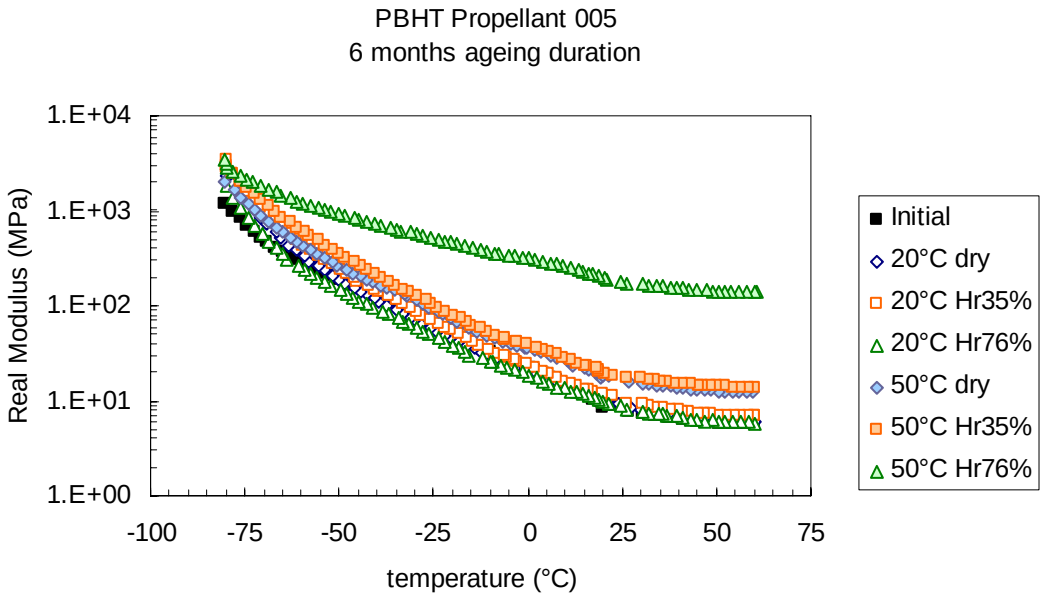

Figure 20 : Real modulus of aged HTPB propellant

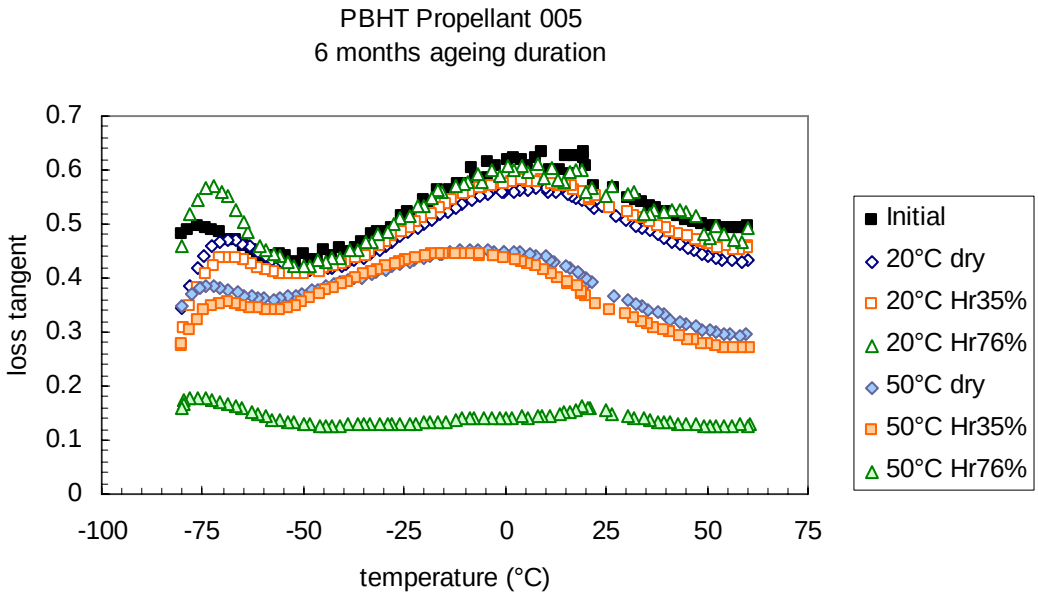

Figure 21 : loss tangent of aged HTPB propellant

It is clearly seen that the material aged at the temperature of +20°C does not present any noticeable modification of its behaviour whatever the ageing conditions are. On the contrary, the ageing temperature of +50°C shows a spectacular mechanical behaviour modification which may be resumed as a material rigidification. This stiffness increase is amplified by the relative humidity value and results in a modulus increase together with a loss tangent decrease. The behaviour could then be compared to the material in its glassy state. It should also be pointed out that the broad loss tangent peak which is centered around +10°C in the unaged condition tends to move towards low temperature after ageing. There is no doubt that the material macromolecular structure is deeply modified by the ageing process though no well identified mechanism may be refered to. This glassy behaviour will of course strongly affect the crack propagation behaviour as it will be demonstrated later on.

4.2 Uniaxial tension

It is useless saying that the aged material behaviour is observed in uniaxial tension tests. Only a single crosshead rate (115mm/min) at room temperature condition is applied due to the lack of material but these tests gives a important picture of the modified behaviour.

The figure 22 shows this modified behaviour for each ageing condition.

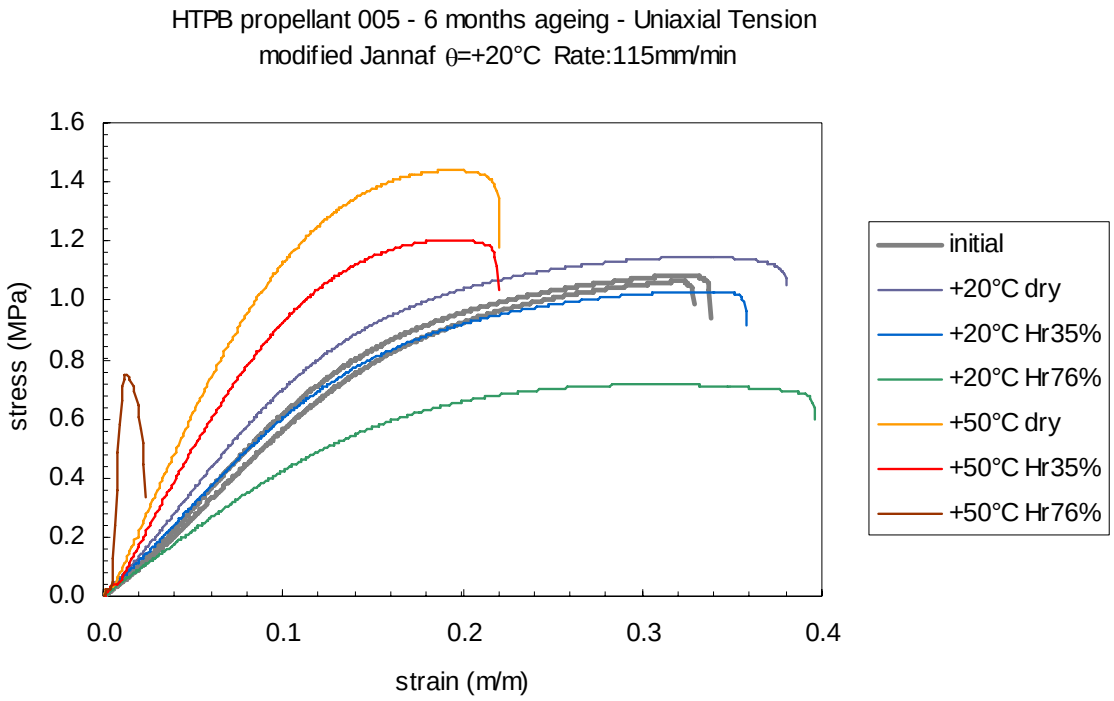

Figure 22 : Uniaxial tension tests for aged propellant

This figure shows that the material is unmodified for room temperature and slight humidity condition (Hr35%) but becomes a bit stiffer when the ageing condition is dry. Again, for this temperature (+20°C) and for the higher humidity (Hr76%) condition, the material becomes weaker both in terms of rigidity and capacity. For the hot temperature ageing condition (+50°C) the material exhibits an imporant stiffness increase with a retardation effect due to the presence of a slight humidity. Finaly for both the high temperature and high humidity ageing condition the material behaviour modification is spectacular betrayed by a very high modulus and a important capacity loss. The underlying physical mechanisms responsible for this behaviour are not clear but it is worthnotting that this modification in the tensile behaviour are accompagnied by a noticeable change in the loss tangent.

Table 5 reminds all the properties extracted from these results.

ageing duration	ageing temp.	relative humidity	test temp.	strain rate	E_{tg}	S_m	e_m	e_r
months	°C	%	°C	min^{-1}	MPa	MPa	%	%
6	+20	dry	+20	1	7.6	1.15	32.5	38.0
6	+20	35%	+20	1	6.4	1.03	32.6	35.6
6	+20	76%	+20	1	4.5	0.71	31.5	39.5
6	+50	dry	+20	1	13.3	1.44	18.8	21.9
6	+50	35%	+20	1	10.9	1.20	18.6	21.8
6	+50	76%	+20	1	143	0.75	0.83	2.33

These figures confirms the general tendencies qualitatively observed on the stress-strain curves. The material aged at room temperature is sensible to humidity with a noticeable decrease in stiffness properties for high moisture values, a constant behaviour for the medium range value of this parameter and a slight increase in dry conditions. The picture is very different for the high temperature ageing with a global increase of the stiffness for the medium and dry humidity condition and a brittle behaviour for the combination of high temperature and high humidity.

4.3 Crack propagation tests

The crack propagation tests are performed using the same operating conditions as for the unaged material but the uncracked sample was not tested again for material saving purposes. The results are presented for each temperature and geometry (SENT and PS samples) on figures 23,24,25 and 26.

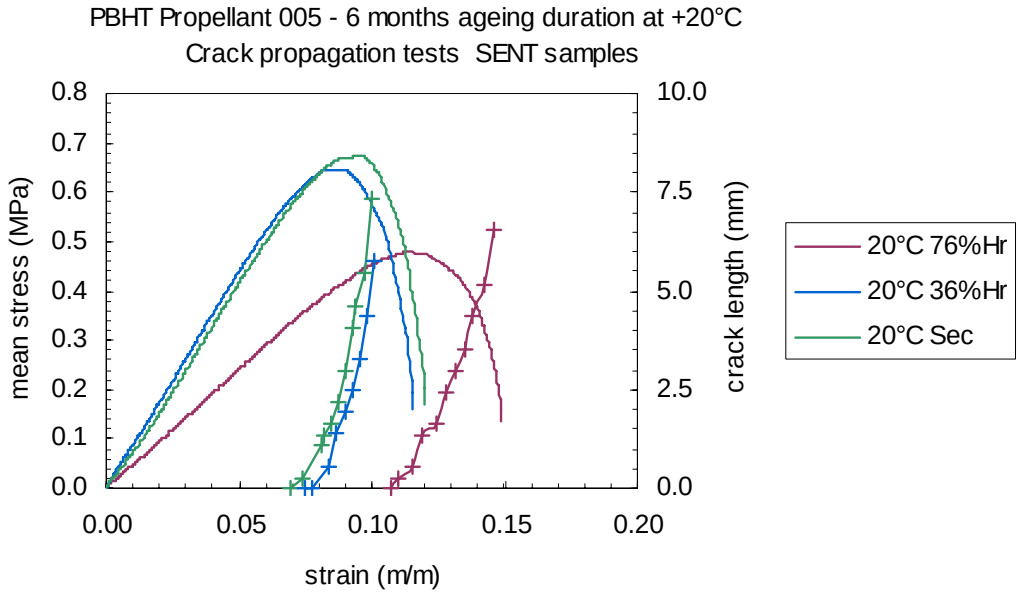

Figure 23 : Crack propagation test for SENT samples (+20°C ageing condition)

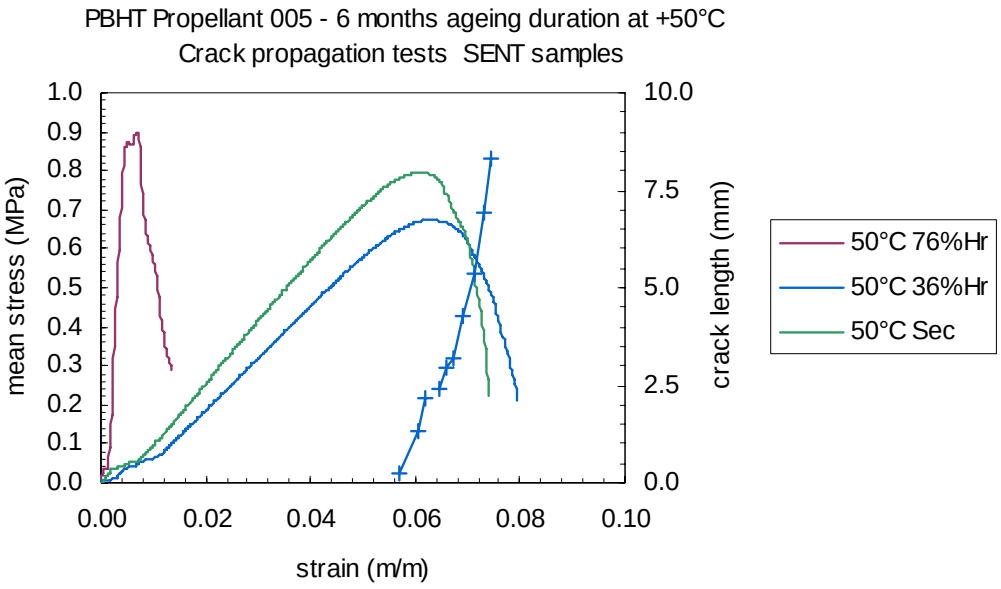

Figure 24 : Crack propagation test for SENT samples (+50°C ageing condition)

The crack propagation velocity for the sample aged at +50°C and Hr76% was to high for the video recorder to catch a meaningfull image and for the aged material in dry air the recording operation unfortunately failed. This is why no crack length measure is available for these two conditions. Anyway, this lack of informations on the kinetics of crack propagation does not exclude the calculation of the critical stress intensity factor.

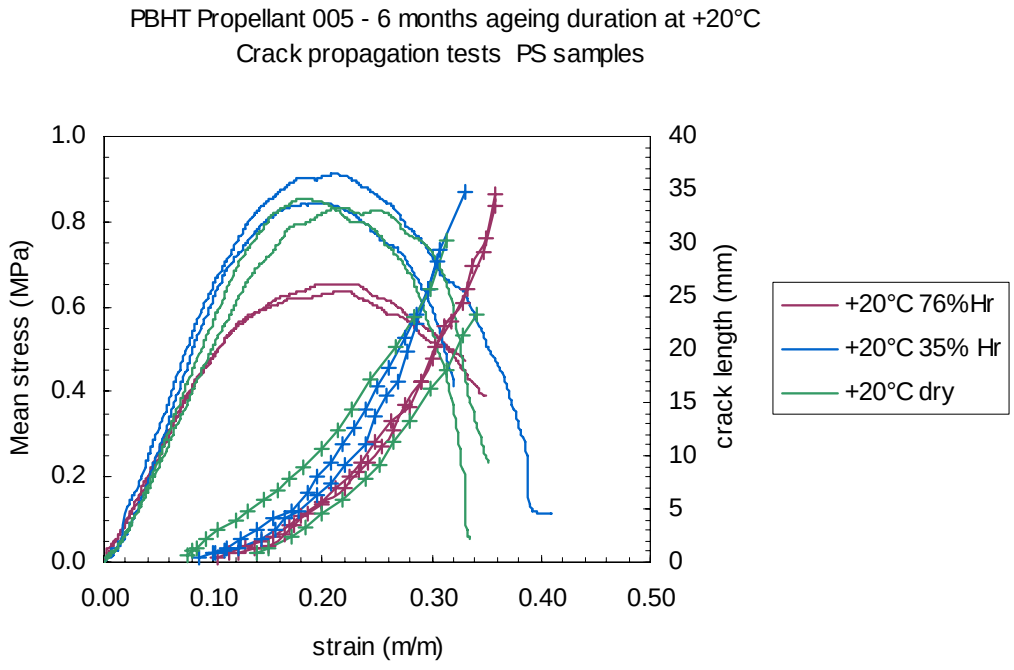

Figure 25 : Crack propagation test for PS samples (+20°C ageing condition)

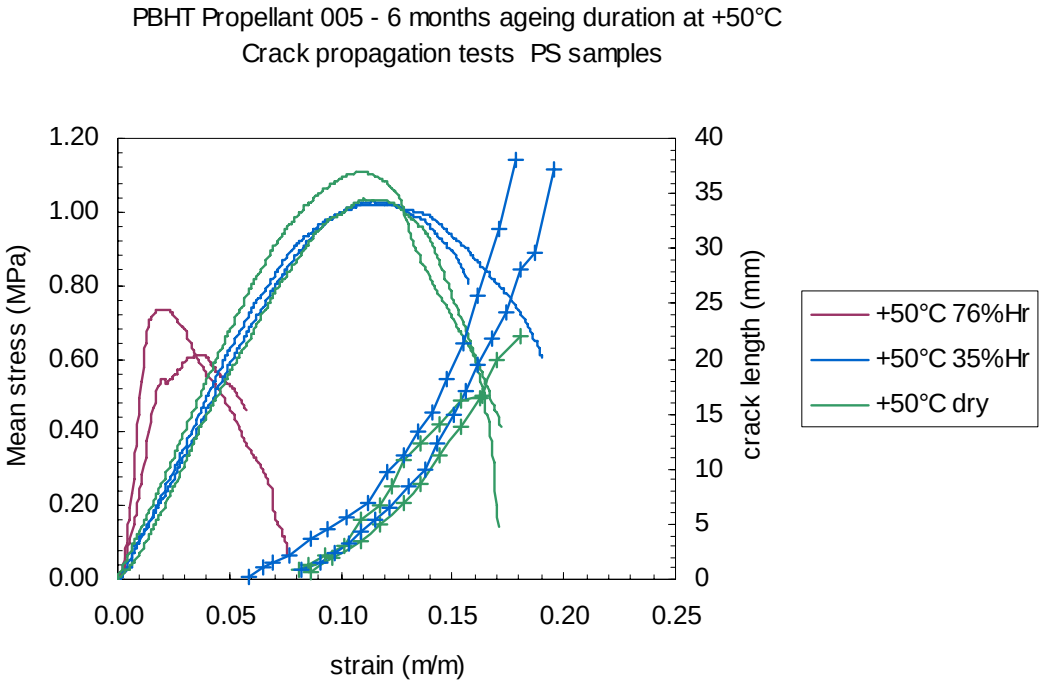

Figure 26 : Crack propagation test for PS samples (+50°C ageing condition)

As for the SENT samples, the PS experiment for the +50°C and Hr76% ageing exhibits such a brittle material behaviour that the recording of the crack propagation was not possible with the video. However in this case the maximum stress was chosen as the crack initiation point.

The table 6 reminds all the material properties extracted from these tests.

ageing condition		sample	a_0	h_0	σ_c	K_{1c}	E	G_c
temp.	Hr		mm	mm	MPa	MPa√m	MPa	mJ/mm²
20	dry	SENT	6	110	0.456	0.070	7.6	0.647
20	35%	SENT	6	110	0.490	0.075	6.4	0.886
20	76%	SENT	6	110	0.360	0.055	4.5	0.682
50	dry	SENT	6	110	0.552	0.085	13.3	0.542
50	35%	SENT	6	110	0.492	0.076	10.9	0.525
50	76%	SENT	6	110	0.734	0.113	143	0.089
20	dry	PS	35	21	*0.419*	*0.037*	*7.6*	*0.181*
20	dry	PS	35	21	0.689	0.061	7.6	0.492
20	35%	PS	35	21	0.633	0.056	6.4	0.493
20	35%	PS	35	21	0.578	0.051	6.4	0.411
20	76%	PS	35	21	0.553	0.049	4.5	0.536
20	76%	PS	35	21	0.495	0.044	4.5	0.429
50	dry	PS	35	21	1.030	0.091	13.3	0.628
50	dry	PS	35	21	0.876	0.078	13.3	0.454
50	35%	PS	35	21	0.681	0.060	10.9	0.335
50	35%	PS	35	21	0.929	0.082	10.9	0.624
50	76%	PS	35	21	0.734	0.065	143	0.030
50	76%	PS	35	21	0.609	0.054	143	0.020

Table 6 : crack propagation properties for aged material

It should be emphasis that the crack propagation velocity is not supported by the analysis of results since no simple physical model is availbale. Nevertheless it can be seen on these figures that the crack speed increases with the material stiffness as could be expected from an energy restitution analysis.

In terms of toughness properties, the results shows some systematic differences between the SENT and PS geometries probably due to the non linear behaviour which is not taken into account in the fracture mechanics relations. It should be emphasis that the brittle material properties (+50°C Hr76%) does not appear clearly from the K1c figures (the values are about the same or even higher for the SENT specimen) since this properties involves only the stress value. On the contrary, the fracture energy which invelves a rigidity notion via the modulus, exhibits very clearly this behaviour.

Finaly, it is noticed that the influence of the ageing process is about the same as oberved in uniaxial tension. The +20°C ageing conditions leads to rather unchanged fracture properties (note the softening by 76% humidity is compensed by the retardation of the crack propagation onset) while the +50°C condition leads to a material tougness increase except for the Hr76% condition.

5. Conclusions

The mechanical behaviour of an HTPB propellant is described with the objective of a crack propagation modelization. To provide the necessary properties involved in the viscoelastic model addressed the material is characterized with various tests. The firts of them is the classical mechanical spectrometry from which the shifting factors are extracted for a ulteriour utilization in the master curves constructions. These master curves concerns mainly the tensile properties gathered at various strain rates and temperatures. To allow an insight in the hyperelastic behaviour the material is also tested in simple shear from which in addition to uniaxial results some Mooney-Rivlin law fitting has been performed. Though this informations are not used in conventional incompressible description, the volumetric component of the behaviour has been observed for three strain rates.

The aim of the program being the crack propagation behaviour these tests were conducted for two samples geometry namely, Single Edge Notch tension and Pure Shear. The fracture mechanics properties derived from the these results shows a coherent picture though some discrepencies are systematicaly observed with these two geometries.